Initial Steps Towards a Clinical FLASH Radiotherapy System: Pediatric Whole Brain Irradiation with 40 MeV Electrons at FLASH Dose Rates

Dylan Yamabe Breitkreutz[a], **Muhammad Shumail**[d], **Karl K. Bush**[a], **Sami G. Tantawi**[b,d], **Peter G. Maxim**[e,1], **Billy W. Loo Jr.**[a,c,1]

[a]Department of Radiation Oncology, Stanford University, Stanford, California;

[b]Department of Particle Physics and Astrophysics, Stanford University, Stanford, California;

[c]Stanford Cancer Institute, Stanford University, Stanford, California;

[d]SLAC National Accelerator Laboratory, Stanford University, Menlo Park, California;

[e]Department of Radiation Oncology, Indiana University, Indianapolis, Indiana

Abstract

In this work, we investigated the delivery of a clinically acceptable pediatric whole brain radiotherapy plan at FLASH dose rates using two lateral opposing 40-MeV electron beams produced by a practically realizable linear accelerator system. The EGSnrc Monte Carlo software modules, BEAMnrc and DOSXYZnrc, were used to generate whole brain radiotherapy plans for a pediatric patient using two lateral opposing 40-MeV electron beams. Electron beam phase space files were simulated using a model of a diverging beam with a diameter of 10 cm at 50 cm SAD (defined at brain midline). The electron beams were collimated using a 10-cm-thick block composed of 5 cm of aluminum oxide and 5 cm of tungsten. For comparison, a 6-MV photon plan was calculated with the Varian AAA algorithm. Electron beam parameters were based on a novel linear accelerator designed for the PHASER system and powered by a commercial 6-MW klystron. Calculations of the linear accelerator's performance indicated an average beam current of at least 6.25 µA, providing a dose rate of 115 Gy/s at isocenter, high enough for cognition-sparing FLASH effects. The electron plan was less homogenous with a homogeneity index of 0.133 compared to the photon plan's index of 0.087. Overall, the dosimetric characteristics of the 40-MeV electron plan were suitable for treatment. In conclusion, Monte Carlo simulations performed in this work indicate that two lateral opposing 40-MeV electron beams can be used for pediatric whole brain irradiation at FLASH dose rates of >115 Gy/s and serve as motivation for a practical clinical FLASH radiotherapy system, which can be implemented in the near future.

---

[1]Address for correspondence: Dept. of Radiation Oncology, Stanford University School of Medicine, 875 Blake Wilbur Dr., Stanford, CA 94305; bwloo@stanford.edu. Department of Radiation Oncology, Indiana University School of Medicine, 535 Barnhill Dr., RT 041, Indianapolis, IN 46202; pmaxim@iu.edu.

INTRODUCTION

The benefits of FLASH radiotherapy to spare healthy tissues while maintaining effective tumor killing has been demonstrated in a number of different preclinical models (1). Normal tissue sparing by FLASH compared to conventional-dose-rate radiotherapy has been demonstrated for a variety of organ systems (gastrointestinal, brain, skin, lung) (1–6), as well as multiple species (zebrafish, mice, mini-pigs, cats) (1–8), while control of multiple tumor models has remained comparable (lung, breast, head and neck, ovarian, pancreas) (1–8). In 2019 the first human patient was treated for a skin tumor with FLASH using 5.6-MeV electrons, demonstrating favorable tumor control and healthy tissue sparing (7). However, the development of a clinical FLASH system capable for treating typical deep-seated and large volume cancer targets is non-trivial and currently no practical system exists.

Our group is currently developing novel medical linac technology for a pluridirectional high-energy agile scanning electronic radiotherapy (PHASER) system capable of treating cancer with megavoltage (MV) photons at FLASH dose rates (9). A single 10-MV photon beamline is currently being built (to the same specifications as the ultimate multi-beamline PHASER design) for preclinical FLASH radiobiology research, using a linear accelerator structure based on the distributed RF-coupling architecture with genetically optimized cell design (DRAGON) (9, 10) powered by a commercially available 6-MW klystron/modulator RF power source (ScandiNova, Uppsala, Sweden).

In the current work we evaluated the feasibility of repurposing the same accelerator/RF source combination for a "scaled-down" PHASER implementation that could be realized clinically in the near term for selected indications. Although the single 10-MV photon beamline described above will be suitable for preclinical FLASH irradiation of small animals at a relatively short photon source-to-subject distance, different operating parameters would be needed to produce FLASH dose rates for practical clinical scenarios. By treating directly with electrons of sufficiently high energy to produce adequate depth dose, even much lower beam current can produce FLASH dose rates (11–13). Thus, we sought to evaluate an approach of operating this linac at higher accelerating gradient but lower beam current, within the limits of the available RF power source and even though it was not optimized for such parameters.

The configuration evaluated here would deliver treatment with two opposing lateral 40-MeV electron beams (instead of photons) using two accelerators powered by the same common RF power source (Fig. 1A). As a first step in characterizing such a system we used Monte Carlo methods to simulate pediatric whole brain irradiation. This treatment site was chosen as it was suitable for two lateral opposing beams. Additionally, this is a patient population and clinical scenario that would derive the greatest potential benefit of sparing cognitive function postirradiation, which has previously been observed in preclinical experiments with mice when using FLASH in comparison to conventional-dose-rate irradiation (4, 5, 8). We also calculated the beam currents and corresponding dose rates that would be achievable under these operating parameters.

MATERIALS AND METHODS

Dose Calculations

The EGSnrc software packages, BEAMnrc and DOSXYZnrc, were used for all Monte Carlo calculations (14). A CT scan of a pediatric patient was converted into an .egsphant phantom. Hounsfield unit (HU) values were converted to physical densities using a clinical calibration curve. Three materials were included in the phantom: air, water and cranial bone. The HU range corresponding to each material was: −1,000 to −100 HU for air, −100 to 200 HU for water and 200 to 2,000 HU for cranial bone. The phantom's voxel size was $2.5 \times 2.5 \times 2.5$ mm. BEAMnrc was used to model a circular diverging beam with a diameter of 10 cm. The size of the beam was defined at isocenter located at the midplane of the brain at a depth of 7 cm. The beam model included two stacked blocks defined by BLOCK component modules each with a thickness of 5 cm. The first block was made of aluminum oxide (3.95 g/cc) to reduce the energy of the beam with minimal bremsstrahlung photon production and the second block was made of tungsten (19.25 g/cc) to block the remaining transmitted electrons and photons. The block aperture was designed to emulate a standard clinical photon whole brain irradiation setup using an open field extending down to the second cervical vertebrae with blocking for the eyes and oral cavity/oropharynx (Fig. 1B). Two lateral opposing beams were simulated with a source-to-axis (SAD) distance of 50 cm. There was an air gap of 5 cm between the end of the block and the phantom's surface. Each phase space file generated by BEAMnrc has a minimum of 10 million particles including both electrons and bremsstrahlung photons. Phase space files were then input into DOSXYZnrc for dose calculation. The average statistical uncertainty in highest-dose voxels of the dose distributions calculated with DOSXYZnrc was 2%.

For comparison, a 6-MV photon plan was generated in Eclipse. The plan consisted of two lateral opposing beams with open fields that extended down to the second cervical vertebrae with blocking for the eyes and oral cavity/oropharynx using the MLCs. No intensity modulation was used in the photon plan. Dose was calculated using the anisotropic analytical algorithm (AAA) (Varian, Palo Alto, CA) with a dose calculation grid of $2.5 \times 2.5 \times 2.5$ mm with heterogeneity correction turned on.

Monte Carlo-generated .3ddose files and Eclipse-generated DICOM dose files were analyzed using RT_Image (15) and MATLAB (MathWorks® Inc., Natick, MA). Each plan was normalized to deliver 3 Gy to 95% of the brain volume. Dose volume histograms (DVH) were calculated for the brain volume in each plan. Dose homogeneity indices were calculated in accordance with ICRU 83, namely $HI = [D_2 − D_{98}]/D_{50}$ (16).

Beam Current Calculations

The electron beam parameters were based on the DRAGON linear accelerator design currently being built for the preclinical FLASH photon system described above and powered by a commercial 6-MW klystron/modulator RF power source. This linac was designed for ultra-high-dose-rate 10-MV photon irradiation, and as such was optimized for very high electron beam current (beam loading) at 0.3 A peak current and 0.5% duty factor (5 μs pulse

length at 1,000 Hz repetition rate, which is within the performance range of the available RF power source) for an average beam current of 1.5 mA at 10 MeV energy.

We calculated the beam current that would be produced when operating the same linac with a higher gradient to produce a 40-MeV electron beam under the same RF power constraint. To produce the higher gradient, the duty factor (pulse length) can be traded for higher peak power through the use of a pulse compressor, of which compact prototypes conservatively capable of four-fold pulse compression have been built (9, 17, 18). Thus, 24 MW of peak input RF power to the accelerator structure, with 1.25 μs pulse length and 1,000 Hz repetition rate (0.125% duty factor), is assumed in this case. Because the design is not optimized for such operation, a substantial portion of the RF input power will be reflected rather than transferred to the beam.

The PHASER linac (designed for 10-MeV energy, 0.3 A peak current) comprises the following structures:

1. A 5-cell injector (RF coupling coefficient: $\beta_1 = 2.59$, shunt impedance $R_{s1} = 3.64$ MΩ).

2. A 36-cell linac (RF coupling coefficient: $\beta_2 = 3.86$, shunt impedance $R_{s2} = 85.43$ MΩ).

3. A three-port power splitter, which divides the total power of the input port in the ratio of 0.57:3.73 at the two output ports for the five-cell injector and the 36-cell linac, respectively. The relative phases for these two structures are $-30°$ and $-150°$, respectively.

The reflection from each RF structure is given as:

$$|\Gamma_n| = \frac{\beta_n - B_n}{\beta_n + B_n}, \quad B_n = 1 + \frac{P_{bn}}{P_{wn}}, \quad n = \begin{cases} 1, \text{ 5 cell injector} \\ 2, \text{ 36 cell linac} \end{cases}. \tag{1}$$

Here, $|\Gamma_n|$ is the ratio of the field amplitudes of the reflected RF wave from the structure to that of the incident wave. Also, P_{bn} is the power gained by the beam and P_{wn} is the power lost in the walls of the accelerator structure and are given as follows in terms of the beam current I and voltage V_n of the structure,

$$P_{bn} = IV_n, P_{wn} = V_n^2/R_{sn} \tag{2}$$

Using the S-matrix of the three-port splitter with the correct phase along with the above-mentioned relations, we can calculate the various parameters of interest for the 24-MW power at its input port. The results of these calculations are shown in Table 1.

RESULTS

Figure 2A shows dose distributions of the 40-MeV electron plan on the top row and the 6-MV photon plan on the bottom row. The range of displayed dose was 0% to 110%, with the mean brain dose of each plan displayed as 100%. The homogeneity index within the brain of

the 40-MeV electron plan was 0.133 in comparison to the photon plan's index of 0.087. Based on the ICRU definition of homogeneity, a lower value indicates a more homogeneous dose distribution. Figure 2B shows the DVH for the brain volume of each plan. The plans were normalized for 95% coverage of the brain by the prescription dose (3 Gy). The maximum dose in the 40-MeV plan was 3.6 Gy compared to 3.3 Gy in the photon plan.

Table 1 shows the results of the beam current calculations. Here, P_{ref} is the power reflected back from the input of the three-port splitter towards the RF source due to mismatched beam loading conditions. In summary, large gains in beam current are possible with a small compromise in beam energy.

From Table 1, conservatively, 5 mA peak current can be produced at a beam energy of 39.5 MeV. Factoring the RF power system's duty factor of 0.125% results in an average electron beam current of 6.25 μA (total of the two opposing beams). Based on the Monte Carlo model, at this beam current the dose rate at isocenter is 115 Gy/s. Of note, there was no appreciable difference between DVHs or homogeneity of plans produced by beams from 39.2- to 40-MeV electron energy (data not shown).

DISCUSSION

As shown in Fig. 2, the 40-MeV electron plan is slightly less homogeneous than the 6-MV photon plan. The "speckled" appearance of the electron plan is due to electron scattering and is magnified by comparison to the photon plan, which is inherently smoothed by the AAA algorithm. The more quantitative measure of homogeneity, the homogeneity index, indicates that both plans are reasonably similar in this aspect, and are in fact both clinically acceptable. The homogeneity of both the electron and photon plan would improve with intensity modulation.

Raster scanning of the electron beam would be a natural way to achieve both the diverging beam geometry for adequate field size and intensity modulation. Modeling the scanning beam was past the scope of this current investigation.

The dose rate of 115 Gy/s is anticipated based on preclinical studies to be more than high enough to achieve the normal tissue sparing benefits of FLASH, which have been demonstrated at dose rates >40 Gy/s (1, 19). In particular, this dose rate is greater than the observed threshold of ~60 Gy/s for the neurocognitive sparing effect of FLASH (4, 5, 8). As shown in Table 1, by varying the linac parameters, much higher dose rates should be possible with reductions in beam energy small enough to be dosimetrically insignificant. For example, we found no appreciable difference in the plans when the beam energy was reduced from 40 to 39.2 MeV, at which the calculated peak beam current was 20 mA corresponding to a dose rate of 450 Gy/s at the mid-plane of the brain. Thus, even if a simple beam scattering foil is used to produce divergence of the beam, there should be ample current to overcome that inefficiency and maintain FLASH dose rates. Moreover, this performance is achievable despite the linac being optimized for very different operating parameters, and even higher beam current and/or beam energy can be produced for the same RF power if the linac design is optimized accordingly.

We evaluated the feasibility of producing a clinically acceptable pediatric whole brain radiation therapy plan using FLASH 40-MeV electron beams. We anticipate that the same beam configuration would be suitable for other selected clinical scenarios in which parallel opposed beams are often used, e.g., spine or limb radiotherapy. Future directions of this work would include evaluating additional use cases and the performance of linacs specifically optimized for high electron energies in this range.

CONCLUSION

FLASH therapy shows great promise for the treatment of cancer given its ability to spare healthy tissues in comparison to conventional-dose-rate radiotherapy. However, the difficulty of producing treatment beams at the required dose rates to achieve the FLASH effect has been a barrier to the development of a FLASH therapy system capable of treating typical deep-seated and large-volume cancers in humans. This work has preliminarily demonstrated the feasibility of a practically achievable radiotherapy system capable of delivering whole brain irradiation to pediatric patients at FLASH dose rates greater than 100 Gy/s, using an alternative configuration of technology currently being built for preclinical FLASH radiobiology research and therefore realizable in the near future. Such a treatment has the potential to reduce the cognitive decline of pediatric patients after radiation therapy and improve their quality of life. Furthermore, the development of such a system would expand the tools available to the scientific community to more fully assess the potential of FLASH for the treatment of cancer, including that of human patients.

ACKNOWLEDGMENTS

REFERENCES

1. Favaudon V, Caplier L, Monceau V, Pouzoulet F, Sayarath M, Fouillade C, et al. Ultrahigh dose-rate FLASH irradiation increases the differential response between normal and tumor tissue in mice. Sci Transl Med 2014; 6:245ra93.

2. Diffenderfer ES, Verginadis II, Kim MM, Shoniyozov K, Velalopoulou A, Goia D, et al. Design, implementation, and in vivo validation of a novel proton FLASH radiation therapy system. Int J Radiat Oncol Biol Phys 2020; 106:440–8. [PubMed: 31928642]

3. Levy K, Natarajan S, Wang J, Chow S, Eggold JT, Loo P, et al. FLASH irradiation enhances the therapeutic index of abdominal radiotherapy for the treatment of ovarian cancer. bioRxiv 2020.

4. Montay-Gruel P, Petersson K, Jaccard M, Boivin G, Germond J-F, Petit B, et al. Irradiation in a flash: Unique sparing of memory in mice after whole brain irradiation with dose rates above 100 Gy/s. Radiother Oncol 2017; 124:365–9. [PubMed: 28545957]

5. Simmons DA, Lartey FM, Schuler E, Rafat M, King G, Kim A, et al. Reduced cognitive deficits after FLASH irradiation of whole mouse brain are associated with less hippocampal dendritic spine loss and neuroinflammation. Radiother Oncol 2019; 139:4–10. [PubMed: 31253467]

6. Vozenin M-C, De Fornel P, Petersson K, Favaudon V, Jaccard M, Germond J-F, et al. The advantage of FLASH radiotherapy confirmed in mini-pig and cat-cancer patients. Clin Cancer Res 2019; 25:35–42. [PubMed: 29875213]

7. Bourhis J, Sozzi WJ, Jorge PG, Gaide O, Bailat C, Duclos F, et al. Treatment of a first patient with FLASH-radiotherapy. Radiother Oncol 2019; 139:18–22. [PubMed: 31303340]

8. Montay-Gruel P, Acharya MM, Petersson K, Alikhani L, Yakkala C, Allen BD, et al. Long-term neurocognitive benefits of FLASH radiotherapy driven by reduced reactive oxygen species. Proc Natl Acad Sci U S A 2019; 116:10943–51. [PubMed: 31097580]

9. Maxim PG, Tantawi SG, Loo BW Jr. PHASER: A platform for clinical translation of FLASH cancer radiotherapy. Radiother Oncol 2019; 139:28–33. [PubMed: 31178058]

10. Tantawi S, Nasr M, Li Z, Limborg C, Borchard P. Distributed coupling accelerator structures: A new paradigm for high gradient linacs. arXiv 2018 (https://bit.ly/2Egh9TR)

11. Bazalova-Carter M, Liu M, Palma B, Dunning M, McCormick D, Hemsing E, et al. Comparison of film measurements and Monte Carlo simulations of dose delivered with very high-energy electron beams in a polystyrene phantom. Med Phys 2015; 42:1606–13. [PubMed: 25832051]

12. Bazalova-Carter M, Qu B, Palma B, Hardemark B, Hynning E, Jensen C, et al. Treatment planning for radiotherapy with very high-energy electron beams and comparison of VHEE and VMAT plans. Med Phys 2015; 42:2615–25. [PubMed: 25979053]

13. Schuler E, Eriksson K, Hynning E, Hancock SL, Hiniker SM, Bazalova-Carter M, et al. Very high-energy electron (VHEE) beams in radiation therapy; Treatment plan comparison between VHEE, VMAT, and PPBS. Med Phys 2017; 44:2544–55. [PubMed: 28339108]

14. Kawrakow I, Mainegra-Hing E, Rogers D, Tessier F, Walters B. The EGSnrc code system: Monte Carlo simulation of electron and photon transport NRCC Report No. PIRS-701 Ottawa, Canada: National Research Council Canada; 2020.

15. Graves EE, Quon A, Loo BW. RT_Image: an open-source tool for investigating PET in radiation oncology. Technol Cancer Res Treat 2007; 6:111–21. [PubMed: 17375973]

16. International Commission on Radiation Units and Measurements. The ICRU Report 83: prescribing, recording, and reporting photon-beam intensity-modulated radiation therapy (IMRT). J ICRU 2010; 10:1–106.

17. Franzi M, Wang J, Dolgashev V, Tantawi S. Compact rf polarizer and its application to pulse compression systems. Phys Rev Accel Beams 2016; 19:062002–10.

18. Tantawi SG, Nantista CD, Dolgashev VA, Pearson C, Nelson J, Jobe K, et al. High-power multimode X-band rf pulse compression system for future linear colliders. Phys Rev Spec Top Accel Beams 2005; 8:042002–1–19.

19. Vozenin MC, Hendry JH, Limoli CL. Biological benefits of ultra-high dose rate FLASH radiotherapy: Sleeping Beauty awoken. Clin Oncol 2019; 31:407–15.
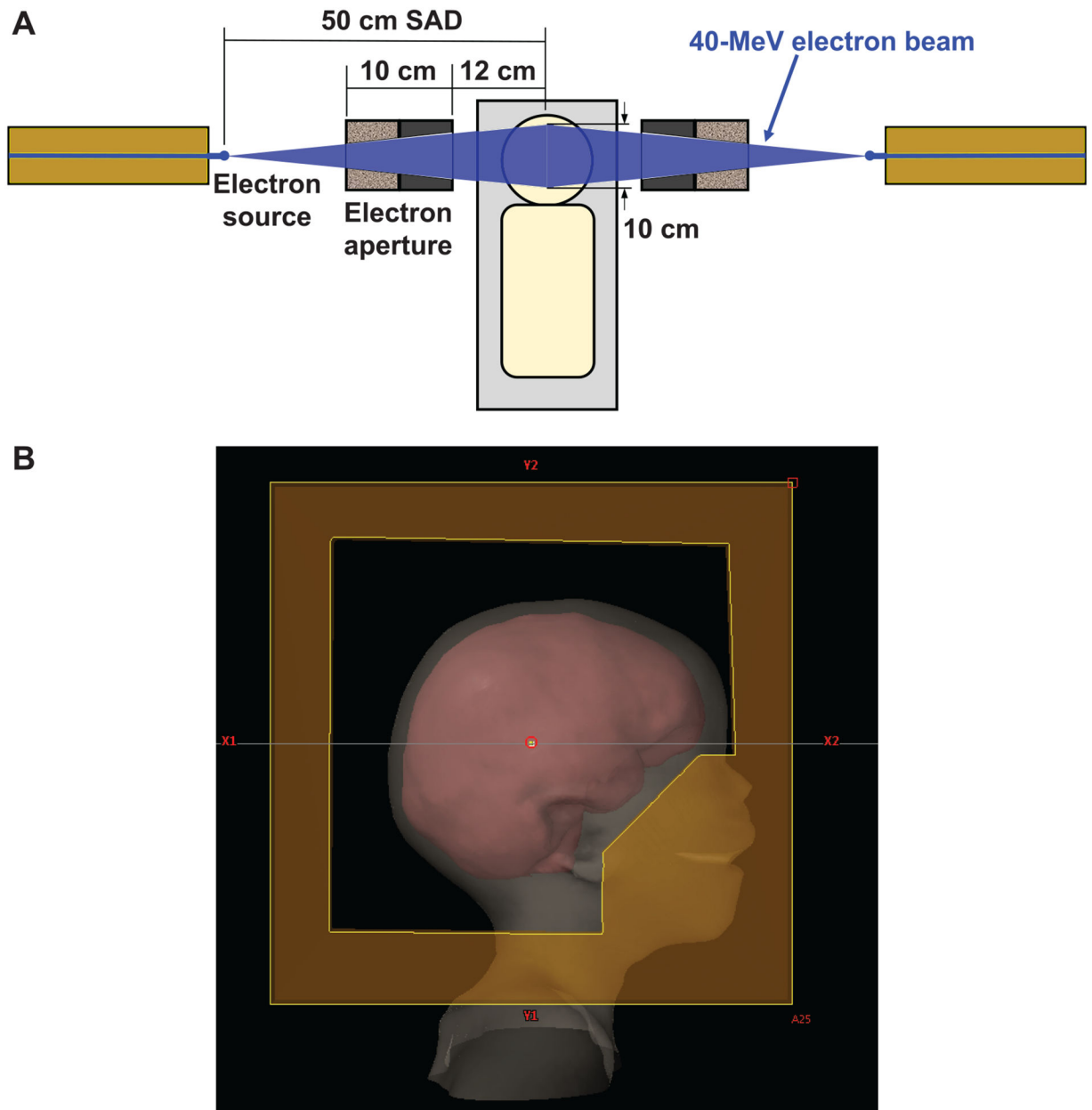
FIG. 1.
Panel A: Schematic of beam arrangement for FLASH 40-MeV electron beams. Panel B: Beam's-eye-view of the right-side electron aperture used in the 40-MeV electron plan.
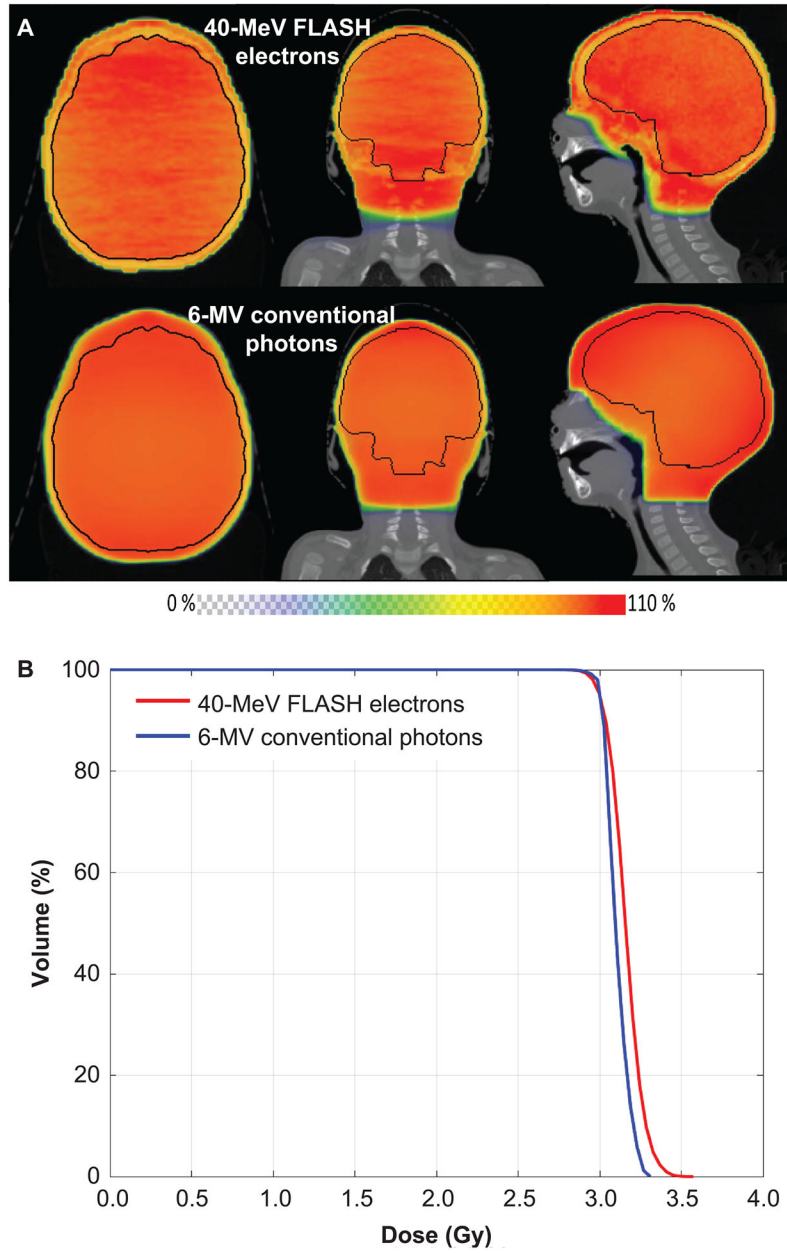
FIG. 2.

Panel A: Dose distributions of 40-MeV FLASH electron plan generated with Monte Carlo (top row) and 6-MV conventional photon plan calculated in Eclipse (bottom row). Panel B: Dose volume histograms of the 40-MeV FLASH electron plan (red) and the 6-MV photon plan (blue) for the brain volume. The plans were normalized for 95% coverage of the brain by the prescription dose (3 Gy). The 40-MeV electron plan is slightly less homogeneous than the 6-MV photon plan (homogeneity index 0.133 vs. 0.087), although both are clinically acceptable.

TABLE 1

Calculated Peak Electron Beam Current vs. Beam Energy under Various Operating Parameters Leading to Varying Amounts of Reflected RF Power

Current I (mA)	Energy (MeV) $e(V_1 + V_2)$	V_1 (MV)	V_2 (MV)	P_{b1} (MW) IV_1	P_{w1} (MW) V_1^2/R_{S1}	P_{b2} (MW) IV_2	P_{w2} (MW) V_2^2/R_{S2}	P_{ref} (MW)
1	39.6	3.28	36.35	0.003	2.95	0.04	15.5	5.56
5	39.5	3.28	36.25	0.016	2.95	0.18	15.4	5.49
10	39.4	3.25	36.14	0.033	2.91	0.36	15.3	5.41
20	39.2	3.23	35.92	0.065	2.86	0.72	15.1	5.25
30	38.9	3.21	35.69	0.096	2.84	1.07	14.9	5.09
50	38.4	3.18	35.23	0.159	2.78	1.76	14.5	4.78
70	37.9	3.14	34.78	0.220	2.71	2.43	14.2	4.48
100	37.2	3.09	34.10	0.309	2.61	3.41	13.6	4.06

Notes. P_{ref} is the power reflected back from the input of the three-port splitter towards the RF source due to mismatched beam-loading conditions, owing to the linac design being optimized for 10-MeV energy rather than ~40 MeV. Large gains in beam current are possible with a small compromise in beam energy, facilitating FLASH dose rates.